

# A STUDY ON MOTION MODE IDENTIFICATION FOR CYBORG ROACHES

Jeremy Cole, Farrokh Mohammadzadeh, Christopher Bollinger, Tahmid Latif,  
Alper Bozkurt, and Edgar Lobaton

Department of Electrical and Computer Engineering  
North Carolina State University, Raleigh, NC 27606, USA

## ABSTRACT

This paper demonstrates the ability to accurately detect the movement state of Madagascar hissing cockroaches equipped with a custom board containing a five degree of freedom inertial measurement unit. The cockroach moves freely through an unobstructed arena while wirelessly transmitting its accelerometer and gyroscope data. Multiple window sizes, features, and classifiers are assessed. An in-depth analysis of the classification results is performed to better understand the strengths and weaknesses of the classifier and feature set. The conclusions of this study show promise for future work on cockroach motion mode identification and localization.

**Index Terms**— cyborg cockroach, inertial measurement, motion recognition

## 1. INTRODUCTION

In a debris-filled disaster environment, it is vital to quickly locate and save trapped people. Traditional search operations often require other individuals to intervene, putting additional lives in danger. In response, we have developed a biobotic insect platform comprised of a Madagascar hissing cockroach (*Gromphadorhina portentosa*) equipped with a battery-powered circuit board which we refer to as a backpack [1] (Figure 1). Previously, these biobots, or cyborg roaches, have been successfully controlled via external commands to move along a desired path [2]. The Madagascar hissing cockroach was the prime choice for several reasons. It is small enough to fit into small crevices while it is also large enough to carry a circuit board with communication and sensing capabilities. Cockroaches are exploratory insects by nature, which is ideal when dealing with a disaster scenario as described. They can be easily reared and are relatively docile while being manipulated. Robotic platforms have difficulties navigating non-uniform terrain while cockroaches are notoriously good at getting around cluttered areas.

To use the electronically-augmented cockroach effectively as a search and rescue agent, we also need a means of

This work was fully funded by the National Science Foundation under the Cyber-physical Systems Program (Award Number 1239243).

localizing it. To do so, we have equipped the cockroach with a custom printed board containing a three-axis accelerometer, a two-axis gyroscope, and a wireless, low-power system-on-chip with a Zigbee radio. For localization purposes, it is critical to be able to determine its movement state. By knowing the type of terrain, physical constraints due to the environment, or mode of locomotion, we can perform more accurate position estimation. Motivated by this, it is our goal to demonstrate that, using only the inertial measurement units (IMUs) mounted on the roach, we can recognize the roach's current mode of motion.

The problem of single-sensor activity analysis has been studied extensively [3, 4, 5]. Sprager et al. [6] show that current techniques are very successful at gait analysis in controlled environments. However, these studies focus on human gait, which is very different from the subject of our study. We have found very few studies that look at the gait of non-human subjects, but one recent effort targeted gait analysis in horses. Using the known characteristics of a horse's gait, Kopniak et al. [7] successfully differentiated between those gaits using inertial sensor data.

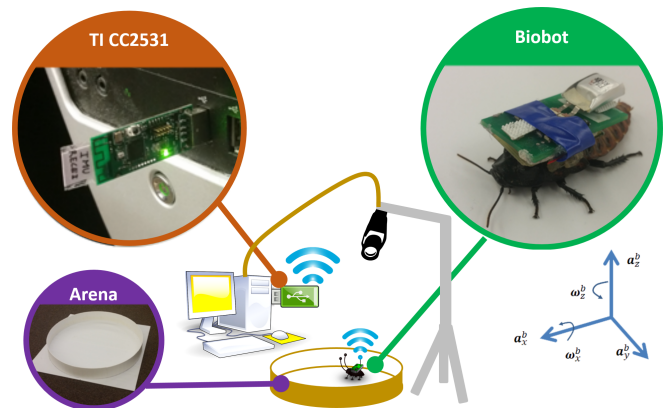


**Fig. 1.** Experimental setup including biobot with sensor backpack. A three-axis accelerometer and two-axis gyroscope are used. The IMU coordinate frame is shown in the figure, where  $\{a_x^b, a_y^b, a_z^b\}$  and  $\{\omega_x^b, \omega_y^b, \omega_z^b\}$  denote the sensitive axes for the accelerometer and gyroscope, respectively.

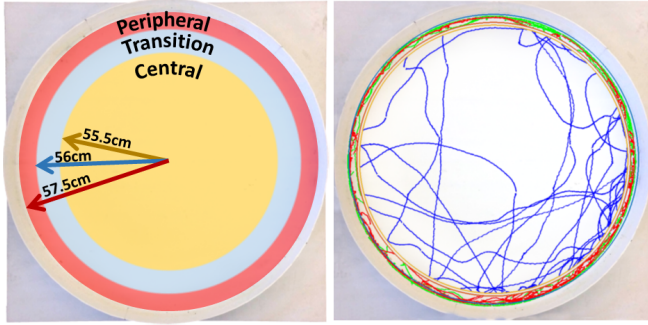


**Fig. 2.** The circular arena used for the experiments. The radii of the peripheral, transition, and central zones are marked accordingly (left). Sample trajectories are shown (right).

There are existing models for roach behavior that are clearly defined under controlled conditions. Jeanson et al. [8] have developed a model for roach motion that alternates between wall-following when near the edges of an obstacle, and a random walk when far away from obstacles. Daltorio et al. [9] have shown that this model also describes the exploratory behavior of roaches in mazes. Given this model of roach activity, we have clear justification for the existence of distinct modes of motion that, taken together, describe a roach’s gait as it explores its environment.

Our approach uses data captured from an inertial measurement sensor mounted on the roach. Using the existing model of roach behavior and standard gait analysis techniques, we have constructed a classification model that accurately predicts the gait, or “motion mode”, of the roach. The rest of the paper is organized as follows: Section 2 details our experimental setup, sensing modalities, and how we establish a ground truth for motion mode estimation; Section 3 explains how we preprocess our IMU data and which features we extract; Section 4 presents the analysis of our classification algorithm; and Section 5 concludes with future work.

## 2. DATA COLLECTION

### 2.1. Experimental Setup

We collected our data using an adult, male Madagascar hissing cockroach. A sensor backpack (Figure 3) containing a TI CC2530 microcontroller, Analog Devices ADXL335 (three-axis accelerometer), and STMicroelectronics LPY410ALTR (two-axis gyroscope), was mounted on the top of the roach’s exoskeleton (Figure 1) for IMU data collection. The backpack was powered by a 50mAh lithium polymer battery, which lasted for about an hour under current experimental conditions.

The purpose of this study was to estimate different modes of motion for roaches. Roaches primarily navigate using their antennae [2], and prefer to follow the contours of objects once

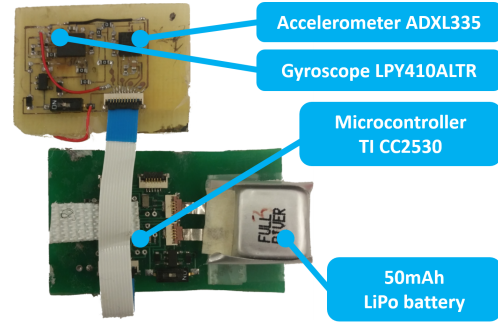


**Fig. 3.** Components in biobot’s sensor backpack.

they detect them, a behavior called wall-following in the literature [8]. We were also interested in discerning when the roach was stationary, as this state is commonly used in inertial navigation, which is one of our main motivations. To this end, we constructed a circular arena (Figure 2) and used it to detect four types of motion: stopped (S), clockwise movement along the arena boundary (CW), counter clockwise movement along the arena boundary (CCW), and movement that is away from the boundary, which we refer to as free movement (FM). Sample signals for each of the four classes are shown in Figure 4.

Jeanson et al. [8] used a circular arena divided into two regions, peripheral and central; we adopted the same nomenclature and added a new zone called the transition zone. For our setup (Figure 2), wall-following is defined to occur when the roach is moving within the peripheral zone and the angle between the roach’s heading and the tangent of the circle is within  $\pm 45^\circ$ . Movement in the transition zone is not

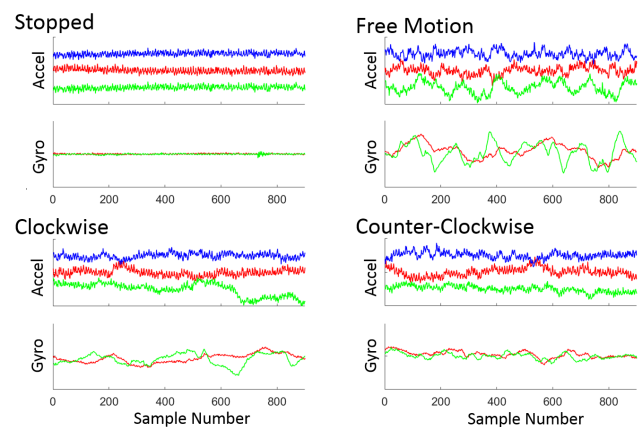


**Fig. 4.** Sample IMU signals are shown for the different motion modes. The accelerometer measurements correspond to  $x$  (red),  $y$  (green) and  $z$  (blue) axis. Signals were vertically shifted so they do not overlap to improve visibility. Gyroscope measurements correspond to  $x$  (green) and  $z$  (red) axis.

used for classification. This was done to better distinguish between wall-following and free movement for classification purposes. We defined the peripheral zone to be three centimeters in width based on our observation of roaches performing wall-following when within this distance. The size of the transition band was set as one centimeter in width.

The IMU data was sampled at an average sampling rate of 900 Hz using the CC2530; the resulting IMU data was sent via ZigBee to a TI CC2531 connected to a computer running MATLAB, which was used to log the IMU data along with its time of arrival. The roach’s movement was tracked using a Microsoft LifeCam HD-3000, operating at 30 frames per second. The IMU data and video data were synchronized by tapping the IMU board three times in succession every 10-15 minutes to create instantaneous events that could be clearly observed in the video data and in the IMU data. We excluded the IMU data affected by these synchronization taps from the analysis.

## 2.2. Ground Truth

We used a visual tracking system to establish the ground truth, which necessitated a means of synchronizing video frames to IMU samples. To accomplish this, we performed a least-squares optimization over the aforementioned sync taps. We assumed a linear fit and minimized the error between the estimated video time of the sync taps, calculated from the arrival time of the IMU data in MATLAB, and the actual sync taps obtained from the video. We further refined the linear fit by using the coefficients to initialize a min-max optimization of the worst sync tap error. We obtained a synchronization error of 0.11 seconds (approx. 4 frames). To account for this synchronization error, we excluded the first and last four frames of an activity when labeling the data. We only used activities lasting at least one second to ensure that activities had enough samples for classification.

## 3. METHODS

We preprocessed our data using a Hampel Filter (e.g. [10]) to remove outliers without affecting the rest of the data. We chose to segment our data using a sliding window approach with no overlap. In the literature it is common to use window sizes of several seconds [11]; however the majority of these studies are for human activity recognition and it is not apparent if these window sizes would be suitable for roaches. After testing various window sizes, we found that 1.5 seconds was sufficient for classification.

### 3.1. Feature Extraction

We used features commonly found in the literature for our feature vector. These features are listed in Table 1 and described below.

The first four statistical moments (mean, variance, skewness, kurtosis) are commonly used on time series data as features. These features were calculated for each of the five sensor axes (Figure 1). The correlation between sensor axes has been found to be useful for detecting movement along a single dimension [12]. As such, we checked the correlation between each of the five sensors. Lara and Labrador [13] reported that measures of statistical dispersion, such as MAD and IQR, are widely used on IMU signals. As an additional dispersion measure, we checked the range, which is the peak-to-peak value. Skog et al. [14] derived a test statistic for distinguishing between stationary and moving data. They experimentally showed that gyroscope energy is especially effective at determining whether an IMU is moving. Therefore, we incorporated the energy of each of the gyroscopes as temporal features.

Fourier coefficients are effective at distinguishing between different types of ambulatory activities [6] when analyzed over the frequency band containing the gait cycle. We used the Fast Fourier Transform to get the Fourier coefficients in the 0-10Hz band and calculate the power spectral density (PSD) over this band for each of the sensors. It is possible for different forms of movement to have the same PSD, so we also used spectral entropy [17] and the magnitude of the Fourier coefficients along each axis as features.

Wavelets can be used to extract temporal-frequency information about a signal. Unlike the windowed Fourier Transform, which captures frequency vs. a fixed window size (i.e. time scale), wavelets resolve frequency into time scales that become increasingly smaller with decomposition level. This property can be used to perform fractal analysis on a signal and obtain its fractal dimension, a measure of how much the signal repeats over varying time scales. This feature has been used to differentiate between different types of ambulatory activities [16]. The energy of the wavelet coefficients at varying decomposition levels has also been used [17]. We calculated the Fractal dimension and the wavelet coefficient energy, at each of the first five decomposition levels, for every sensor using a Daubechies wavelet of order 5.

**Table 1. Feature Vector**

Group (# Features)	Name (# Features)	Reference
Temporal (47)	mean(5), variance(5), skewness(5), kurtosis(5), range(5), Gyro Energy(2), Correlation between Axes(10), Mean Absolute Deviation (MAD)(5), Interquartile Range (IQR)(5)	[11, 13, 15]
Spectral (40)	Average Power Spectral Density(5), Magnitude of Fourier Coefficients(30), Spectral Entropy(5)	[16, 5, 17]
Wavelet (30)	Wavelet Coefficient Energy(25), Wavelet Fractal Dimension(5)	[16, 18]

### 3.2. Feature Classification

We analyzed the performance of our feature vector using four commonly used classifiers in the literature: Support Vector Machines (SVM), Random Forests (RF), Linear Discriminant Analysis (LDA), and k-Nearest Neighbor (kNN) [6, 11, 17]. We chose to implement a linear SVM using a one vs. all approach to classification. LDA, RF, and kNN, are multi-class classifiers, so a selection strategy is not needed for multi-class classification. We used LDA with a loss function that assigned equal weight to erroneous classifications, RF was implemented with 50 trees, and kNN was implemented with  $k$  equal to the square root of the number of training samples [19]. All classifiers were implemented using MATLAB.

## 4. RESULTS

Various options for selecting the best window size, the best set of features, and the best classification algorithm are available. A comprehensive list of each of these parameters was created and narrowed down to a more manageable size. Four window sizes were selected of durations 0.5s, 1.0s, 1.5s, and 2.0s. We have three groups of features: Temporal (FT), spectral (FS), and wavelet (FW). From these three groups which were previously shown in Table 1, we assessed all seven possible combinations: Each of the three sets alone (FT, FS, FW), all pairwise combinations (FTS, FTW, FSW), and all three sets combined (FTSW). Lastly, we used SVM, RF, LDA, and kNN as the classifiers. To compare the classification capability of these methods, we crossvalidated each configuration using a 10-fold partition of our dataset. To determine which mix of window size, feature set, and classifier yields the best predictions, we combinatorially compared the classification results using each predictor’s average Macro (M) F1 score for comparison [20]. The M F1 score is obtained by taking the harmonic mean of the M precision and the M recall, which in turn are obtained from the mean of the individual means of each class’s precision and recall. Other statistical measures include the average accuracy, macro precision, and macro recall. Ultimately, the optimal combination that produced the best classification result (via highest F1 score) was a 1.5s window using all features and the SVM classifier. Table 2 shows the precision of each class along with the normalized misclas-

**Table 2.** Precision Matrix

		Predicted			
		S	FM	CW	CCW
Ground Truth	S	0.9315	0	0.0093	0.0055
	FM	0.0548	0.7669	0.0926	0.0609
	CW	0.0137	0.1805	0.8759	0.0416
	CCW	0	0.0526	0.0222	0.8920

**Table 3.** Performance under varying window size

Window Size	0.5s	1.0s	1.5s	2.0s
Average Accuracy	0.9123	0.9290	0.9302	0.9336
M Precision	0.8168	0.8450	0.8666	0.8531
M Recall	0.8118	0.8535	0.8603	0.8476
F1 Score	0.8143	0.8492	0.8634	0.8503

**Table 4.** Performance under varying feature set

Feature Set	FT	FS	FW	FTS	FTW	FSW	FTSW
Average Accuracy	0.9185	0.9125	0.8371	0.9262	0.9222	0.9157	0.9302
M Precision	0.8305	0.8313	0.7074	0.8581	0.8450	0.8355	0.8666
M Recall	0.8354	0.8281	0.7031	0.8502	0.8422	0.8350	0.8603
F1 Score	0.8329	0.8297	0.7052	0.8542	0.8437	0.8352	0.8634

**Table 5.** Performance under varying classifier

Classifiers	SVM	RF	LDA	KNN
Average Accuracy	0.9302	0.9238	0.9226	0.9081
M Precision	0.8666	0.8470	0.8530	0.8255
M Recall	0.8603	0.8437	0.8405	0.8292
F1 Score	0.8634	0.8454	0.8467	0.8274

sification for this result.

For analysis, we evaluated the performance of the approaches as we varied one parameter from the configuration with the best outcomes. For example, Table 3 shows how window size affects classification performance while using SVM and considering all features. Similarly, Tables 4 and 5 vary the feature set and the classifier respectively.

The data show that the Free Moving (FM) class has an unusually high false negative and false discovery rate compared to the other three classes. This is probably best explained by the fact that the cockroach’s gait in the Free Moving (FM) class is similar to that of the Peripheral walking (CW and CCW) classes, making it difficult to distinguish.

## 5. CONCLUSION

We have presented a framework for classifying motion modes for Madagascar Hissing cockroaches. By utilizing standard features and classifiers, we were able to accurately predict when the cockroach is stationary and distinguish between clockwise and counter-clockwise wall-following. Future work will focus on lowering the false positive rate associated with free movement and wall-following by designing new features and making use of graphical models to enforce temporal consistency. The classifier will also be incorporated into an inertial navigation system for the roaches.

## 6. REFERENCES

- [1] A. Bozkurt, E. Lobaton, and M. Sichiitiu, "A biobotic distributed sensor network for under-rubble search and rescue," *Computer*, vol. 49, no. 5, pp. 38–46, 2016.
- [2] T. Latif and A. Bozkurt, "Line following terrestrial insect biobots," in *2012 Annual International Conference of the IEEE Engineering in Medicine and Biology Society*. IEEE, 2012, pp. 972–975.
- [3] L. Chen, J. Hoey, C. Nugent, D. Cook, and Z. Yu, "Sensor-based activity recognition," *IEEE Transactions on Systems, Man, and Cybernetics, Part C (Applications and Reviews)*, vol. 42, no. 6, pp. 790–808, 2012.
- [4] I. Bisio, F. Lavagetto, M. Marchese, and A. Sciarrone, "Comparison of situation awareness algorithms for remote health monitoring with smartphones," in *2014 IEEE Global Communications Conference*. IEEE, 2014, pp. 2454–2459.
- [5] P. Gupta and T. Dallas, "Feature selection and activity recognition system using a single triaxial accelerometer," *IEEE Transactions on Biomedical Engineering*, vol. 61, no. 6, pp. 1780–1786, 2014.
- [6] S. Sprager and M. Juric, "Inertial sensor-based gait recognition: a review," *Sensors*, vol. 15, no. 9, pp. 22089–22127, 2015.
- [7] P. Kopniak and K. Bocian, "Differentiating horse walk and trot on the basis of inertial motion capture," in *2016 9th International Conference on Human System Interactions (HSI)*. IEEE, 2016, pp. 270–276.
- [8] R. Jeanson, S. Blanco, R. Fournier, J. Deneubourg, V. Fourcassié, and G. Theraulaz, "A model of animal movements in a bounded space," *Journal of Theoretical Biology*, vol. 225, no. 4, pp. 443–451, 2003.
- [9] K. Daltorio, B. Mirlletz, A. Sterenstein, J. Cheng, A. Watson, M. Kesavan, J. Bender, R. Ritzmann, and R. Quinn, "How cockroaches employ wall-following for exploration," in *Conference on Biomimetic and Biohybrid Systems*. Springer, 2014, pp. 72–83.
- [10] R. Pearson, "Outliers in process modeling and identification," *IEEE Transactions on Control Systems Technology*, vol. 10, no. 1, pp. 55–63, 2002.
- [11] S. Preece, J. Goulermas, L. Kenney, D. Howard, K. Meijer, and R. Crompton, "Activity identification using body-mounted sensors a review of classification techniques," *Physiological Measurement*, vol. 30, no. 4, pp. R1, 2009.
- [12] D. Figo, P. Diniz, D. Ferreira, and J. Cardoso, "Pre-processing techniques for context recognition from accelerometer data," *Personal and Ubiquitous Computing*, vol. 14, no. 7, pp. 645–662, 2010.
- [13] O. Lara and M. Labrador, "A survey on human activity recognition using wearable sensors," *IEEE Communications Surveys & Tutorials*, vol. 15, no. 3, pp. 1192–1209, 2013.
- [14] I. Skog, P. Handel, J. O. Nilsson, and J. Rantakokko, "Zero-velocity detection—an algorithm evaluation," *IEEE Transactions on Biomedical Engineering*, vol. 57, no. 11, pp. 2657–2666, Nov 2010.
- [15] A. Avci, S. Bosch, M. Marin-Perianu, R. Marin-Perianu, and P. Havinga, "Activity recognition using inertial sensing for healthcare, wellbeing and sports applications: A survey," in *Architecture of computing systems (ARCS), 2010 23rd international conference on*. VDE, 2010, pp. 1–10.
- [16] S. Preece, J. Goulermas, L. Kenney, and D. Howard, "A comparison of feature extraction methods for the classification of dynamic activities from accelerometer data," *IEEE Transactions on Biomedical Engineering*, vol. 56, no. 3, pp. 871–879, 2009.
- [17] F. Attal, S. Mohammed, M. Dedabrishvili, F. Chamroukhi, L. Oukhellou, and Y. Amirat, "Physical human activity recognition using wearable sensors," *Sensors*, vol. 15, no. 12, pp. 31314–31338, 2015.
- [18] T. Leauhatong, N. Nuttaitanakul, and B. Prapochanang, "Optimal selection of mother wavelet for classifying human activities from acceleration signals," in *2015 8th Biomedical Engineering International Conference (BMEiCON)*. IEEE, 2015, pp. 1–5.
- [19] R. Duda, P. Hart, and D. Stork, *Pattern classification*, John Wiley & Sons, 2012.
- [20] M. Sokolova and G. Lapalme, "A systematic analysis of performance measures for classification tasks," *Information Processing & Management*, vol. 45, no. 4, pp. 427–437, 2009.